Neuroscience Research 193 (2023) 20–27

Contents lists available at ScienceDirect

Neuroscience Research

journal homepage: www.sciencedirect.com/journal/neuroscience-research

An open-source application to identify the three-dimensional locations of electrodes implanted into the rat brain from computed tomography images

Mikuru Kudara [a], Nobuyoshi Matsumoto [a,b,*], Nahoko Kuga [a,c], Kotaro Yamashiro [a], Airi Yoshimoto [a], Yuji Ikegaya [a,b,d,*], Takuya Sasaki [a,c,*]

[a] Graduate School of Pharmaceutical Sciences, The University of Tokyo, Tokyo 113–0033, Japan
[b] Institute for AI and Beyond, The University of Tokyo, Tokyo 113–0033, Japan
[c] Department of Pharmacology, Graduate School of Pharmaceutical Sciences, Tohoku University, 6–3 Aramaki-Aoba, Aoba-Ku, Sendai 980–8578, Japan
[d] Center for Information and Neural Networks, National Institute of Information and Communications Technology, Suita City, Osaka 565–0871, Japan

ARTICLE INFO

Keywords:
Computed tomography
Electrodes
Rat
Electrophysiology
Application

ABSTRACT

Electrophysiological recordings using metal electrodes implanted into the brains have been widely utilized to evaluate neuronal circuit dynamics related to behavior and external stimuli. The most common method for identifying implanted electrode tracks in the brain tissue has been histological examination following post-mortem slicing and staining of the brain tissue, which consumes time and resources and occasionally fails to identify the tracks because the brain preparations have been damaged during processing. Recent studies have proposed the use of a promising alternative method, consisting of computed tomography (CT) scanning that can directly reconstruct the three-dimensional arrangements of electrodes in the brains of living animals. In this study, we developed an open-source Python-based application that estimates the location of an implanted electrode from CT image sequences in a rat. After the user manually sets reference coordinates and an area from a sequence of CT images, this application automatically overlays an estimated location of an electrode tip on a histological template image; the estimates are highly accurate, with less than 135 μm of error, irrespective of the depth of the brain region. The estimation of an electrode location can be completed within a few minutes. Our simple and user-friendly application extends beyond currently available CT-based electrode localization methods and opens up the possibility of applying this technique to various electrophysiological recording paradigms.

1. Introduction

In neuroscience research, electrophysiological recordings from implanted metal electrodes in the brain of rodents engaging in various behaviors have unveiled neuronal activity patterns at the high temporal-resolution associated with cognitive, emotional, and mnemonic functions. Recent studies have addressed further challenges by developing high-density arrays of electrodes for large-scale recordings from multiple distributed brain areas (Viventi et al., 2011) and by improving stereotactic surgical techniques for accurate localization of electrodes in deep brain regions such as the piriform cortex, ventral hippocampal CA1 region, and basolateral nucleus of the amygdala (Manabe et al., 2011; Miyawaki and Mizuseki, 2022; Tao et al., 2022). These recent research trends have increased the demand for efficient experimental techniques to determine the three-dimensional spatial locations of electrodes in the brain. However, the current standard procedure to identify the positions of implanted electrodes relies strongly on postmortem histological verifications: euthanizing and decapitating animals, sectioning the brain, staining slices with Nissl staining, and matching individual slices to a brain histology atlas. The locations of implanted electrodes thus remain unknown until long-term experiments are completed, and errors are discovered only by end-point histological assessment. Moreover, these histological techniques require a significant time investment (generally taking days to weeks), and electrode tracks can be altered by damage to brain tissue during the removal of electrode bundles from the brain.

To more directly and noninvasively visualize metal electrodes implanted into the brains of living animals, several methods using computed tomography (CT) scanning and magnetic resonance imaging (MRI) have recently been proposed. These in vivo methods contain no technical issues of postmortem histological verification and enable real-time adjustment of the recording depth using microdrives, as well as the ability to terminate the experiment early if the implant has missed the

* Corresponding authors at: Graduate School of Pharmaceutical Sciences, The University of Tokyo, Tokyo 113–0033, Japan.
E-mail addresses: nobuyoshi@matsumoto.ac (N. Matsumoto), yuji@ikegaya.jp (Y. Ikegaya), takuya.sasaki.b4@tohoku.ac.jp (T. Sasaki).

https://doi.org/10.1016/j.neures.2023.03.003
Received 13 December 2022; Received in revised form 15 March 2023; Accepted 29 March 2023
Available online 30 March 2023

target location. Several studies have reported the benefit of fusing images obtained from MRI and CT scans based on skull landmarks to precisely localize implanted electrodes in the brain in humans (Dalal et al., 2008; Dykstra et al., 2012), monkeys (Miocinovic et al., 2007; Premereur et al., 2020), and rodents (Borg et al., 2015; Rangarajan et al., 2016). This fusion method crucially contributes to the accuracy of the estimates, especially in humans and monkeys, both of which have substantial individual differences in brain size and in the shapes of brain regions. On the other hand, as intact rodent brains have only minor individual differences in structure, CT images alone can estimate electrode locations with a high degree of accuracy comparable to that of MRI fusion methods (Kiraly et al., 2020).

In existing CT-based estimation methods, slice-by-slice image comparisons and matching of electrode locations in CT images to a histology atlas have been performed by manual procedures or custom-made algorithms requiring significant time investment by individual researchers; the widespread and uniform availability of appropriate image processing techniques is a goal that is quite challenging to attain. In this study, we extended previous efforts to utilize CT scanning and developed an open-source Python-based application, termed "CT-matching application", which can automatically match rat CT image sequences to an atlas of histological templates and overlay the locations of implanted electrodes onto the corresponding histological template images. In this paper, we describe the workflow of the application, including definitions of subjective structural features and troubleshooting, and provide representative results from rats with metal electrodes implanted into several brain regions.

2. Materials and methods

2.1. Ethical approval

Animal experiments were performed with the approval of the Animal Experiment Ethics Committee at the University of Tokyo (approval number: P4–4) and according to the ARRIVE guidelines and the University of Tokyo guidelines for the care and use of laboratory animals. Additionally, these experimental protocols complied with the Fundamental Guidelines for Proper Conduct of Animal Experiment and Related Activities in Academic Research Institutions (Ministry of Education, Culture, Sports, Science and Technology, Notice No. 71 of 2006), the Standards for Breeding and Housing of and Pain Alleviation for Experimental Animals (Ministry of the Environment, Notice No. 88 of 2006) and the Guidelines on the Method of Animal Disposal (Prime Minister's Office, Notice No. 40 of 1995). All efforts were made to minimize the animals' suffering.

2.2. Animals

Male and female Wistar rats (SLC, Shizuoka, Japan) were used in this study. Their sex, age, preoperative body weight, and brain weight, are summarized in Table 1. They were housed under conditions of controlled temperature and humidity (22 ± 1 °C, 55 ± 5%) and maintained on a 12:12-h light/dark cycle (lights off from 07:00–19:00) with ad libitum access to food and water. All rats were housed individually before and after experiments.

2.3. Histology of brain tissue to prepare histological template images

To prepare histological template images, a male Wistar rat was perfused intracardially with cold 4% paraformaldehyde (PFA) in 25 mM phosphate-buffered saline (PBS) and decapitated. The whole brain from the prefrontal cortex to the cerebellum was placed in 30% sucrose until equilibrated and then coronally sectioned at a thickness of 55 μm at intervals of 110 μm; the slices were stained with cresyl violet (e.g., Fig. 1E and F). Overall, 114 histological template images were obtained from 5.0 mm anterior (+5.0 mm) to 7.5 mm posterior (–7.5 mm) to bregma.

2.4. Preparation and surgical implantation of electrodes

The electrode array used in this study has been described elsewhere (Okada et al., 2017; Yagi et al., 2018; Konno et al., 2019). Electrodes were nichrome wires with a bare diameter of 25.4 μm bare diameter and a 38.1 μm coated diameter (762000, A-M Systems, WA, U.S.A.), each of which was accommodated in a polyimide tube with a diameter of 300 μm. Five polyimide tubes accommodating the nichrome wires were then bundled in a large polyimide tube with a diameter of 900 μm. Briefly, a plastic core body, custom-made parts created by a 3D printer, metal tubes, electrodes, and an electrical interface board (EIB) (Neuralynx, MT, U.S.A.) were manually assembled so that the tips of the electrodes were located in the targeted brain regions. The other open ends of the electrodes were connected to metal holes in an EIB mounted on top of the core body of the device. All electrical signals from the EIB were transferred to an Omnetics connector. In some experiments, tetrodes were used as electrodes, which were constructed by bundling together four 17 μm polyimide-coated platinum–iridium (90/10%) wires (California Fine Wire, CA, U.S.A.).

The electrodes were implanted using standard surgical procedures similar to those described previously (Okada et al., 2017; Yagi et al., 2018; Konno et al., 2019) (Fig. 1 A). Rats were anesthetized with 1–2% isoflurane gas in air. The rat was then fixed in a stereotaxic instrument with two ear bars and a nose clamp. A craniotomy was created, and an

Table 1
Summary of the sex, age, body weight, brain weight, brain regions (the number of electrodes described in parentheses), and three-dimensional errors between the actual location of an electrode and the location estimated by the application.

Rat ID	Sex (M/F)	Age (weeks)	Body weight (g)	Brain weight (g)	Brain regions (N of electrodes)	Three-dimensional distance (μm) (estimated - actual)
1	M	7 weeks	196	-	Neocortex (2)	0, 117.8
					Hippocampus (1)	134.8
2	M	7 weeks	182	-	Hippocampus (4)	0, 0, 76.4, 110
3	M	7 weeks	188	-	Amygdala (1)	0
					Thalamus (2)	0, 110
					Others (1)	137.4
4	M	8 weeks	210	-	Amygdala (2)	29.7, 58.6
					Thalamus (1)	110
					Others (2)	54.8, 67.5
5	M	16 weeks	280	1.91	Thalamus (1)	95.2
					Others (1)	0
6	M	5 weeks	139	1.61	Neocortex (2)	87.0, 65.2
					Hippocampus (1)	127.9
					Thalamus (1)	21.7
7	F	16 weeks	255	1.74	Hippocampus (2)	45.5, 0
					Others (2)	113.6, 45.5

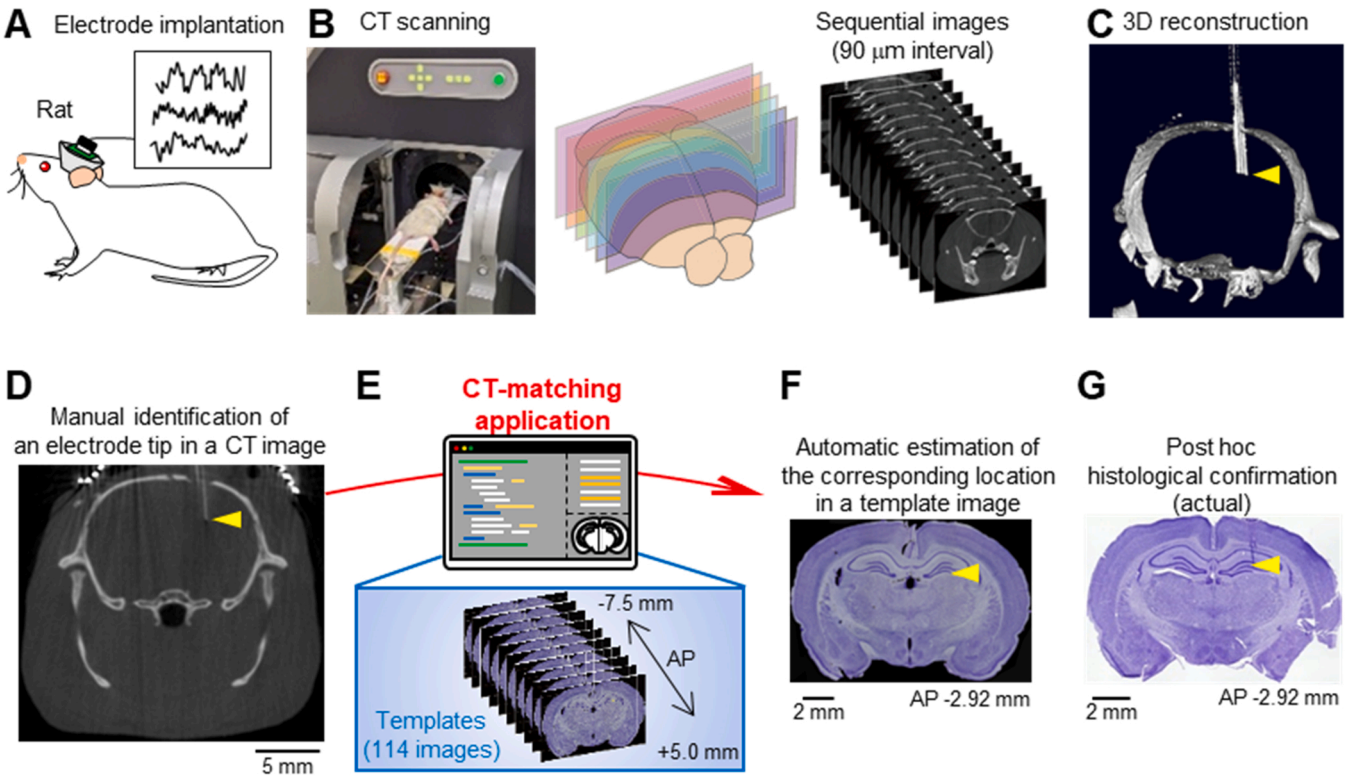

Fig. 1. Estimation of electrode locations from sequential CT images. (A) Electrodes are implanted into a rat to record LFP signals. (B) (Left) A rat with implanted electrodes was subjected to CT scanning. (Middle) Schematic illustrating coronal CT scanning. (Right) Sequential CT images at intervals of 90 μm. (C) A three-dimensional reconstruction of the CT images. The yellow arrowhead indicates an electrode in the brain. (D) A typical image of an electrode tip that was manually identified in a CT image. (E) Based on the manual identification in D, the CT-matching application, which accommodates 114 template images (AP from −7.5 mm to +5.0 mm), automatically estimates the corresponding location of the electrode tip in a histological template image. (F) The location of the electrode tip (indicated by the yellow arrowhead) in a histological template image as estimated by the application in E. (G) A post hoc histological confirmation of the true location of the electrode tip.

electrode was implanted into the right somatosensory cortex (2.2 mm posterior and 3.0 mm lateral to bregma, 2.5 mm from the surface), the right hippocampus (2.8 mm posterior and 3.0 mm lateral to bregma, 3.5 mm from the surface), the right amygdala (1.7 mm posterior and 2.0 mm lateral to bregma, 7.0 mm from the surface), or the left hypothalamus (2.0 mm posterior and 3.0 mm lateral to bregma, 8.0 mm from the surface). After all surgical procedures were performed, the anesthesia was terminated, and the rats were spontaneously allowed to awake from the anesthesia. Following surgery, each rat was housed under daily observation in a standard environment with free access to water and food.

2.5. *In vivo electrophysiology*

One week after the surgery, electrophysiological recordings commenced. The EIB on the animal's head was connected to a Cereplex μ digital headstage (Blackrock Microsystems, UT, U.S.A.), and the digitized signals were transferred to a Cereplex Direct data acquisition system (Blackrock Microsystems). Recordings were performed in the home cage in a dark room. For all recordings, electrophysiological signals (local field potentials (LFPs)) were amplified and digitized at 2 kHz and filtered between 0.1 Hz and 500 Hz.

2.6. *CT scan*

After the electrophysiological recordings, each rat was anesthetized with isoflurane gas and subjected to CT scanning. Three-dimensional images were obtained with an X-ray microcomputed tomography system (CosmoScan GXII, Rigaku, Tokyo, Japan) (Fig. 1B–1D). The parameters for X-ray tomography were as follows: *tube voltage*, 90 kV; *tube current*, 88 μA; *absorbed dose*, 106 mGy; *FOV* (*field of view*), 45 mm; *voxel size*, 90 μm (isotropic); and *scan time*, 2 min. Images were digitized at a slice interval of 90 μm.

2.7. *Histological examination of brain tissue after LFP recordings to confirm electrode locations*

After the electrophysiological recordings, the rats were perfused intracardially with cold 4% PFA in 10 mM PBS and decapitated. The electrodes were carefully removed from the brain 3–5 h after perfusion, and the brains were placed in 30% sucrose until equilibrated, then coronally sectioned at a thickness of 50 μm. The slices were stained with cresyl violet. The true position of the electrode tip was confirmed by identifying the corresponding electrode track in histological tissue sections (Fig. 1 G).

2.8. *Overview of the CT-matching application*

The application stores 114 histological template images at the anterior-posterior coordinates of −7.5 mm to + 5.0 mm relative to bregma. In an application window, the user defines a reference CT image, selects a reference area that surrounds the brain tissue on a CT image, and clicks the location of the electrode tip on the CT image to generate a histological template image showing the estimated location of the electrode tip.

2.9. Preparation of operating environments in Windows

Before starting, an operating environment needs to be prepared. The Python scripts and related files for this application are freely available at https://github.com/UT-yakusaku/CT_matching_app. The following are typical preparatory steps to run the application on Python on a Windows computer.

1. Install "opencv-python", "pydicom", "tifffile", "keyboard", and "numpy" libraries into Python (version 3.7.3 or more) using "pip".
2. Copy "config.py", 'lib.py", and "Electrode_localizer.py" into a main working directory (Fig. 2A).
3. In the main directory, create an "images" folder and put a "templates" folder including all histological template image files (in.tif format) in the "images" folder (Fig. 2A).

Note: One can skip Steps 2 and 3 above by downloading and extracting the GitHub repository.

2.10. Processing of CT image files

After CT images are obtained from a rat, the following steps can be performed in the application to estimate the location of an electrode tip implanted in the brain.

1. Create a folder (for example, "DCMfile" folder) in the "images" folder and put all CT image files (.dcm) obtained from a rat in the "DCMfile" folder (Fig. 2 A).
2. In the "DCMfile" folder, find a "Reference" CT image by visual inspection, e.g., using File Explorer (Fig. 2B; for more details, see the next paragraph and Fig. 3 A and 3B).
3. Open the "config.py" (Fig. 2 C). In the "config.py", write the path for the folder including the CT image files (e.g., "dicom_file_path = './images/DCMfile'"), the path for the folder including the histological template image files (e.g., "template_file_path = './images/templates'"), the number of the reference CT image in the CT files (e.g., "image_ref = 124″), and the total AP length of CT images corresponding to the total length of all of the histological template images (110 μm × 113 = 12.43 mm) ("image_length = 138″ is recommended as 12.43 mm/90 μm (CT scan interval) = 138).
4. Open command prompt, change the working directory to the main directory, and input "python Electrode_localizer.py" to launch "Electrode localizer" (Figs. 2D and 2E).
5. In "Electrode localizer", flip sequential CT images by scrolling the mouse wheel (or pressing "." or "," keys on the keyboard) and find a CT image containing an electrode tip (Fig. 2E).
6. Manually define a "reference rectangle" surrounding the brain tissue (Fig. 2 F, cyan rectangle) by clicking two of its diagonally opposed corners (the first and second clicks on this window; for

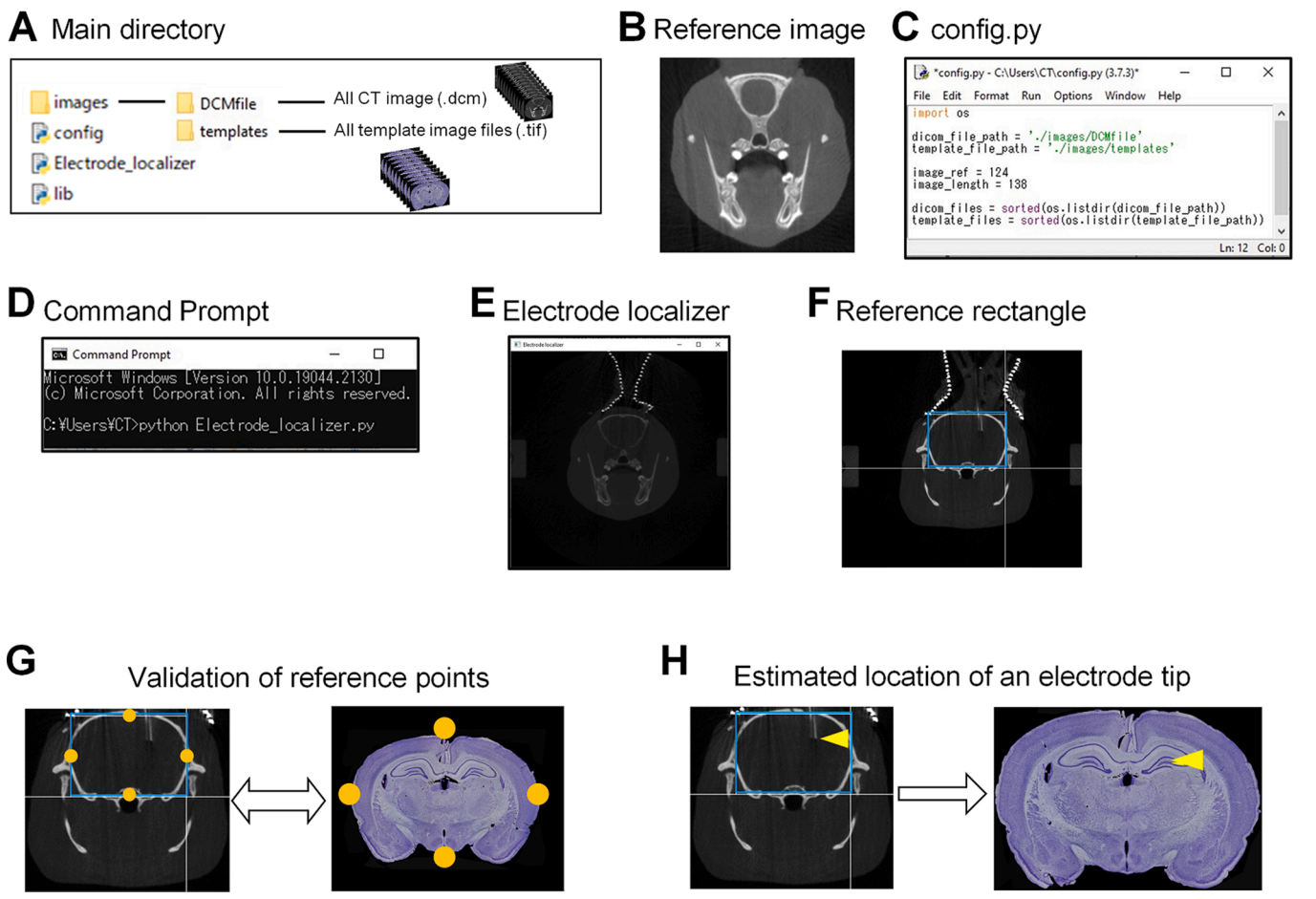

Fig. 2. Procedures in the CT-matching application. (A) A screen image showing the composition of the main directory. (B) A typical reference CT image. (C) A command window for "config.py". (D) A command prompt window. (E) An "Electrode localizer" window. (F) A typical reference rectangle (cyan) created on a CT image containing an electrode tip. (G) (Left) Four reference points (orange) placed along the reference rectangle on a CT image. (Right) Estimation results for the reference points on a histological template image. (H) (Left) An electrode tip marked within the reference rectangle on a CT image. (Right) The estimated location of the electrode tip on a histological template image.

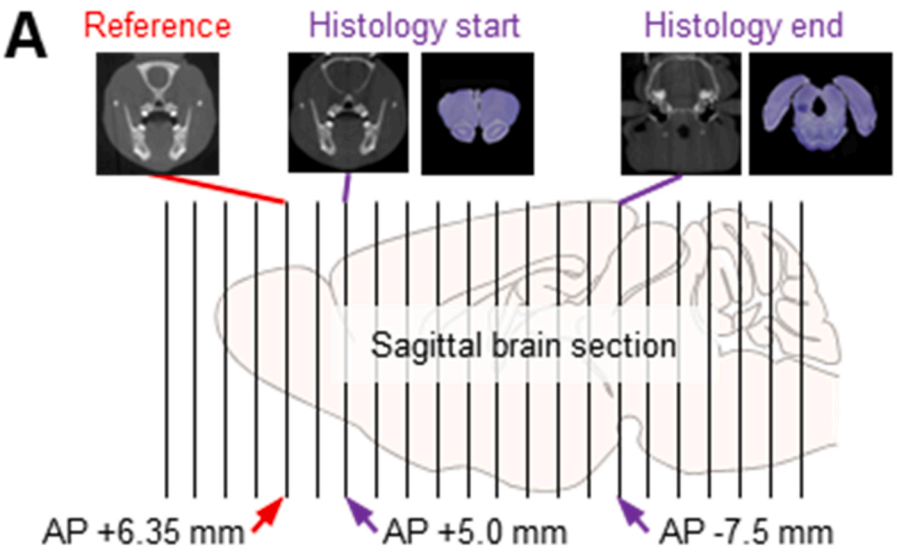

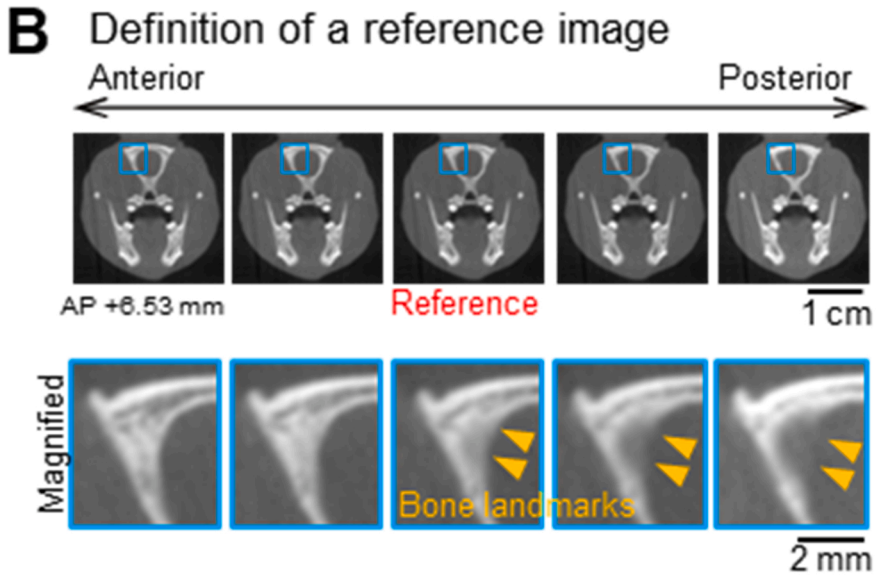

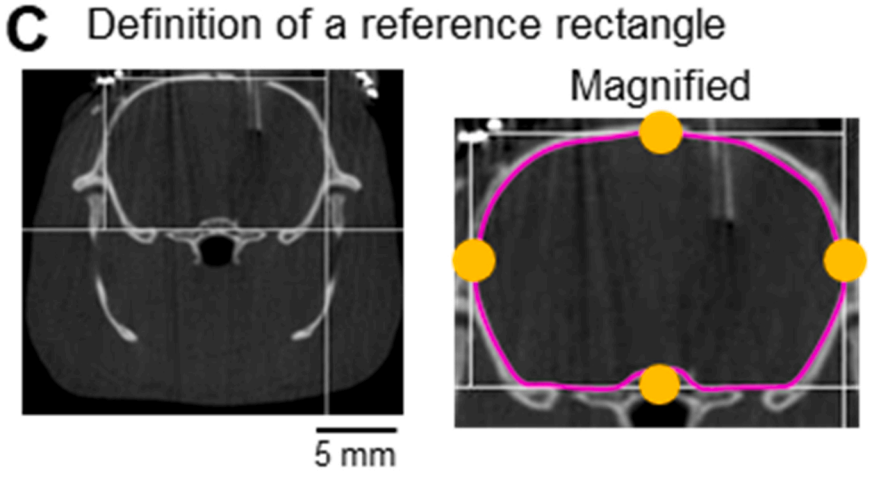

Fig. 3. Details for manual definition of references in CT images. (A) Schematic illustration showing approximate coordinates of a reference CT image and the starting and ending histological images accommodated in the application, superimposed on a sagittal brain section. (B) Definition of a reference CT image (Step 2 in Fig. 2B). The blue areas in the top panels are magnified in the bottom panels. The CT images are viewed from anterior to posterior, and a reference CT image is defined when the bony landmark (corresponding with the upper skull area surrounding the olfactory bulb) indicated by the orange arrowheads begins to thin. (C) Definition of a reference rectangle along the cerebral parenchyma. In the application, this rectangle is created by clicking two of its diagonally opposed corners. The rectangle is magnified in the right panel. The individual edges of the rectangle correspond to the lines of best fit passing through the positions giving the largest cerebral parenchyma volume (indicated by the magenta line). Four reference points on the reference rectangle are indicated by the orange dots.

more detail, see the next paragraph and Fig. 3 C). Note: Moving to a different image eliminates the reference rectangle.)
7. Within the same image, click on a location within the reference rectangle to open a new window showing a histological template image with the corresponding location marked.
8. To confirm that the setting position and size of the reference rectangle are valid, click an edge of the rectangle as a reference point (Fig. 2 G, orange dot) to open a new window showing an estimate of the clicked location in a histological image and ensure that the estimated point is correctly located at the edge of the brain image. Repeat this process for all four edges of the reference rectangle. (Critical step: If the estimated location of a reference point is misaligned in histological template images, reset the rectangle.) (Critical step: Note that this is the most crucial step in the protocol, as it is necessary to verify the accurate alignment of the reference points.)
9. Click the location of the electrode tip (Fig. 2H, yellow arrowhead).
10. The application automatically shows the estimated position of the electrode tip, marked with a yellow arrowhead in a histological template image. Note: Based on the coordinates of the four vertices of the reference rectangle in the CT image, the application automatically scales the size of the CT image within the reference rectangle so that it corresponds to that of the histological template image. Using the scaled image, the estimated location of the electrode tip is automatically determined in the template image.
11. Press the "q" key or close "Electrode localizer" to terminate the application.

2.11. Manual identification of a reference CT image and a reference rectangle

As Step 2 in the processing of CT image files, in a sequence of CT images from a rat in a "DCMfile" folder, a reference CT image that is located approximately 6.35 mm anterior to bregma (Fig. 3 A) needs to be identified by visual inspection. We chose this coordinate as a reference CT image because it has skull features that can be easily identified by any experimenter (Fig. 3B); these features can serve as a subjective criterion to register the AP coordinate of the slice in the application. To identify a reference CT image, for example, using File Explorer on a Windows computer, inspect sequential CT images from anterior to posterior at coordinates of approximately 5.5–7.0 mm anterior to bregma and find a few CT images in which upper bone structures surrounding the olfactory bulb (indicated by the orange arrowheads in Fig. 3B) gradually become thinner. This procedure may include going back and forth to inspect several CT images. When inspecting from the anterior end, define a reference CT image when the bone structure first begins to thin. If CT images do not show perfectly symmetrical structure, the hemisphere containing the implanted electrode of interest should be utilized.

Another manual step is the creation of a reference rectangle along the cerebral parenchyma in a CT image containing the target electrode (Step 6 for processing of CT image files) (Fig. 3 C). Define the individual edges of the rectangle as the lines of best fit passing through the points where the volume of the cerebral parenchyma becomes largest. After creating a reference rectangle, confirm its accuracy by selecting four reference points on the edges of the rectangle in the CT image (Fig. 2 G, orange dots) and comparing them to the corresponding locations on the histological template image (Step 8 for processing of CT image files). The perfect alignment of all of the reference points to the histological template images is crucial for precise localization of electrode locations in subsequent processes. In the case of misalignment, the step of creating a reference rectangle needs to be repeated. Inaccurate reference setting can occur irrespective of the anterior-posterior coordinates.

3. Results

An experienced operator performed surgeries to implant electrodes into various brain regions, including the neocortex, hippocampus, amygdala, and hypothalamus, in rats (Fig. 4 A). After >7 days of postsurgical recovery, LFP signals were recorded from individual brain areas (Fig. 4 A, right), and CT scanning was performed at 90-μm resolution to visualize the implanted electrodes in the rats. These scans clearly identified the tips of electrodes with a diameter of ~50 μm (nichrome wires: 38.1 μm; tetrodes: four 17 μm wires twisted as a bundle). On the other hand, the tip of non-metal silicon-based probes (e.g., A1×32–6 mm-100–177, NeuroNexus) could not be identified. The locations of individual electrodes were differentiated between with an interelectrode distance of 300 μm. According to the procedures for the CT-matching application (see Materials and Methods), the locations of the electrode tips in CT images were localized and visualized on a histological template image (indicated by the yellow arrowheads in Fig. 4 A, middle). In total, all procedures, including the resetting of reference CT images, took no more than a few minutes per rat. To confirm the accuracy of our in vivo localization, we performed standard postmortem histology (i.e., decapitation, brain slicing, and Nissl staining) and identified the locations of the electrode tips in the slices. We first performed analyses from 4 male rats as standard rats with body weight of 182–210 g (Rats #1–4). The detailed brain regions in these rats are summarized in Table 1. For quantification, we calculated the mean difference between each true location identified in a histological slice and the corresponding estimated location in a histological template image along the dorsal–ventral (DV), medial–lateral (ML), and anterior–posterior (AP) axes (Fig. 4B). Here, we manually adjusted the size of the histological slice containing the electrode tip to the size of the corresponding histological template image and calculated the distance between the actual location and the estimated location in the two images. In the DV and ML directions, the average deviation of estimated locations from true locations was 11.5 μm and −1.1 μm, ranging from –82.4–102.3 μm (median = 0 μm) and from –117.8–87.7 μm (median = 0 μm), respectively ($n = 16$ electrodes). These distances were not correlated with the depth of electrodes ($r = –0.30$, $P = 0.26$ (in the DV direction) and $r = 0.06$, $P = 0.81$ (in the ML direction)). In the AP direction, the coordinate of the estimated histological image matched that of the true histological image in 12 out of 16 electrodes, whereas the remaining 1 and 3 electrodes showed estimated images with a deviation of one slice (= 110 μm) anterior and posterior to the true histological image, respectively. These results confirm that our initial adjustment of a reference CT image based on the skull structure at approximately 5.0 mm anterior to the bregma was almost perfectly accurate in estimating the AP coordinates of implanted electrodes. Overall, the two-dimensional distance (in a DV–ML plane) of all rats, computed from these distances on the individual axes, was within 135 μm of the target (Fig. 4 C), which is considerably smaller than one part of a single cortical or subcortical region. These results suggest that the estimation accuracy provided by our application is sufficient to determine whether implanted electrodes are located within the target brain regions.

In addition, we performed the same experiments and analyses from larger male (Rat #5, 16 weeks, 280 g), smaller male (Rat #6, 5 weeks, 139 g), and female (Rat #7, 16 weeks, 255 g) rats. All the results are summarized in Table 1, showing that the three-dimensional distance between the actual location of an electrode and the location estimated by the application was within 130 μm, which was shorter than or almost comparable to that observed from the standard rats. These results suggest that our application is applicable to relatively larger and small rats (at least from 139 to 280 g), irrespective of sexes, with the same accuracy to estimate the locations of implanted electrodes.

4. Discussion

Several methods have been proposed for visualizing electrode tracks

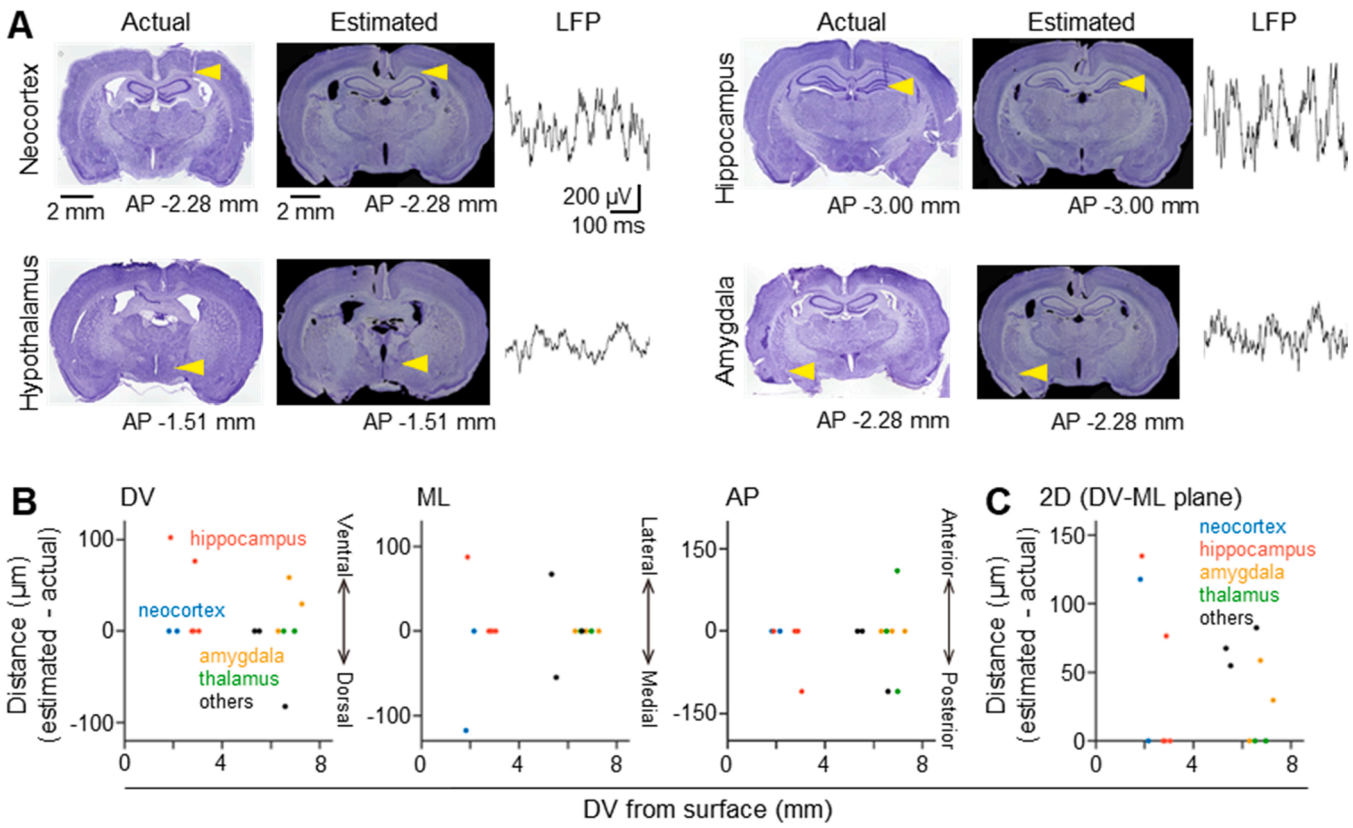

Fig. 4. Comparisons of actual and estimated electrode locations on histological images. (A) Results of representative experiments from four brain regions. Each panel shows an actual electrode location indicated by the yellow arrowhead (left), the corresponding electrode location estimated by the CT-matching application (middle), and an LFP trace recorded from the electrode. Note that the AP coordinates were determined based on a standard brain atlas (Paxinos and Watson, 2013). (B) Distance between the actual location of an electrode and the location estimated by the application along the dorsal–ventral (DV, left), medial–lateral (ML, middle), and anterior–posterior (AP, right) axes, plotted against its dorsoventral distance from the surface; note that 0 μm indicates the surface, while larger values in μm signify more ventral positions. The values in the AP axis were discrete, as the interval between the template images was 110 μm. Each dot shows one experiment, and the dots are labeled in different colors representing the corresponding brain regions ($n = 2$, 5, 3, 3, and 3 electrodes from 4 male rats with body weight of 182–210 g (Rats #1–4)). (C) The distances shown in B were converted to two-dimensional distances in a DV-ML plane.

in the whole rodent brain without slicing the brain tissue; these methods include postmortem tissue clearing and selective plane illumination microscopy or serial block-face two-photon microscopy (Liu et al., 2021), postmortem CT scanning (Benovitski et al., 2022), and CT scanning of animals before the electrodes are removed from the brain (Borg et al., 2015; Bikovsky et al., 2016; Yoshimoto et al., 2022). In particular, fast feedback by CT scanning from living animals to identify implanted electrodes has many advantages over a conventional histological assessment: it enables confirmation of the success of electrode implantation, further adjustment of electrode depth to reach a target region, or early termination of recordings in the case of mistargeting, all of which contribute to identifying potential causes of failure and increasing the throughput of experiments. Recently, CT equipment has become more readily accessible at many universities and research institutes.

In this study, we developed a new application that estimates the anatomical location of metal electrodes from a sequence of CT images of an intact rat brain. This application runs in Python with subjective criteria and takes no more than a few minutes to complete the estimation of an electrode position. Comparisons of these estimated locations to those confirmed by a general histological analysis revealed that the estimates were less than 100 μm from the actual values in most of our experiments (Fig. 4 C), irrespective of the depth of targeted brain regions from the brain surface. This accuracy is sufficiently precise to adapt to the small deep-brain nuclei of the rodent brain, which measure approximately 0.5 mm in diameter.

The quality of our application is crucially limited by the spatial resolution of CT scanning. While we showed that the spatial resolution of 90 μm in our CT scans provided adequate accuracy in the majority of brain regions, this level of resolution was not sufficient to clearly identify thinner nonmetal electrodes (e.g., silicon probes) or differentiate individual electrodes within an electrode bundle with an interelectrode distance of less than 90 μm. Differentiation of implanted objects at a finer scale requires CT systems with higher spatial resolution. This application, in its present form, is designed only for rats and not applicable to mice. While we demonstrated that both male and female rats with body weight from 139 to 280 g can be reliably analyzed, the size and positioning of brain areas may vary in the other types of rats. In that case, the number of histological template images ("image_length"; Step 3 for processing of CT image files) from a reference CT image may be adjusted so that the last histological template image corresponds to the end of the CT image, as shown in Fig. 3 A. In addition, confirmation of four reference points on a reference rectangle (Steps 6–8 for processing of CT image files) may be repeated until the estimated points are correctly located on the four edges of the brain in the corresponding histological template image. If all of the reference points are perfectly aligned, our application will accurately localize electrode locations even for different types of rats. Overall, the application provides substantial improvements in the accurate anatomical localization of metal electrodes, accomplishing the process in a more efficient and user-friendly manner than currently available CT-based localization techniques.

CRediT authorship contribution statement

M.K., N.M., Y.I., and T.S. designed the study. N.K. and T.S. acquired and analyzed the histological data. M.K., K.Y., and A.Y. performed electrode implantation and CT identification. M.K. and N.M. performed the analyses of CT data and prepared the figures. M.K., N.M., and T.S. wrote the main manuscript text. N.M., Y.I., and T.S. supervised the project, and all the authors reviewed the main manuscript text.

Declaration of Competing Interest

The authors declare no competing interests.

Data availability

No data was used for the research described in the article.

Acknowledgments

We thank Tomu Hirata for his technical assistance. This work was supported by funds from the Exploratory Research for Advanced Technology (JPMJER1801) from the Japan Science and Technology Agency (JST), the AMED Strategic International Brain Science Research Promotion Program (18dm0307007h0001), and the Institute for AI and Beyond of the University of Tokyo to Y. Ikegaya; by a KAKENHI grant (20K15926) from the Japan Society for the Promotion of Science (JSPS) to N. Matsumoto; and by KAKENHI grants (21H05036, 21H05243) from the JSPS, funds from the Core Research for Evolutional Science and Technology (JPMJCR21P1) and funds from the Moonshot Research and Development Program (JPMJMS2292) from the JST to T. Sasaki.

References

Benovitski, Y., Lai, A., Saunders, A., McGowan, C., Burns, O., Nayagam, D., Millard, R., Harrison, M., Rathbone, G.D., Williams, R.A., May, C.N., Murphy, M., D'Souza, W., Cook, M.J., Williams, C., 2022. Preclinical safety study of a fully implantable, subscalp ring electrode array for long-term EEG recordings. J. Neural Eng.

Bikovsky, L., Hadar, R., Soto-Montenegro, M.L., Klein, J., Weiner, I., Desco, M., Pascau, J., Winter, C., Hamani, C., 2016. Deep brain stimulation improves behavior and modulates neural circuits in a rodent model of schizophrenia. Exp. Neurol. 283, 142–150.

Borg, J.S., Vu, M.A., Badea, C., Badea, A., Johnson, G.A., Dzirasa, K., 2015. Localization of metal electrodes in the intact rat brain using registration of 3D microcomputed tomography images to a magnetic resonance histology atlas. eNeuro 2.

Dalal, S.S., Edwards, E., Kirsch, H.E., Barbaro, N.M., Knight, R.T., Nagarajan, S.S., 2008. Localization of neurosurgically implanted electrodes via photograph-MRI-radiograph coregistration. J. Neurosci. Methods 174, 106–115.

Dykstra, A.R., Chan, A.M., Quinn, B.T., Zepeda, R., Keller, C.J., Cormier, J., Madsen, J.R., Eskandar, E.N., Cash, S.S., 2012. Individualized localization and cortical surface-based registration of intracranial electrodes. Neuroimage 59, 3563–3570.

Kiraly, B., Balazsfi, D., Horvath, I., Solari, N., Sviatko, K., Lengyel, K., Birtalan, E., Babos, M., Bagamery, G., Mathe, D., Szigeti, K., Hangya, B., 2020. In vivo localization of chronically implanted electrodes and optic fibers in mice. Nat. Commun. 11, 4686.

Konno, D., Nakayama, R., Tsunoda, M., Funatsu, T., Ikegaya, Y., Sasaki, T., 2019. Collection of biochemical samples with brain-wide electrophysiological recordings from a freely moving rodent. J. Pharm. Sci. 139, 346–351.

Liu, L.D., Chen, S., Hou, H., West, S.J., Faulkner, M., International Brain, L., Economo, M. N., Li, N., Svoboda, K., 2021. Accurate localization of linear probe electrode arrays across multiple brains. eNeuro 8.

Manabe, H., Kusumoto-Yoshida, I., Ota, M., Mori, K., 2011. Olfactory cortex generates synchronized top-down inputs to the olfactory bulb during slow-wave sleep. J. Neurosci. 31, 8123–8133.

Miocinovic, S., Noecker, A.M., Maks, C.B., Butson, C.R., McIntyre, C.C., 2007. Cicerone: stereotactic neurophysiological recording and deep brain stimulation electrode placement software system. Acta Neurochir. Suppl. 97, 561–567.

Miyawaki, H., Mizuseki, K., 2022. De novo inter-regional coactivations of preconfigured local ensembles support memory. Nat. Commun. 13, 1272.

Okada, S., Igata, H., Sasaki, T., Ikegaya, Y., 2017. Spatial representation of hippocampal place cells in a t-maze with an aversive stimulation. Front Neural Circuits 11, 101.

Paxinos, G., Watson, C., 2013. The Rat Brain in Stereotaxic Coordinates 7th Edition.

Premereur, E., Decramer, T., Coudyzer, W., Theys, T., Janssen, P., 2020. Localization of movable electrodes in a multi-electrode microdrive in nonhuman primates. J. Neurosci. Methods 330, 108505.

Rangarajan, J.R., Vande Velde, G., van Gent, F., De Vloo, P., Dresselaers, T., Depypere, M., van Kuyck, K., Nuttin, B., Himmelreich, U., Maes, F., 2016. Image-based in vivo assessment of targeting accuracy of stereotactic brain surgery in experimental rodent models. Sci. Rep. 6, 38058.

Tao, K., Chung, M., Watarai, A., Huang, Z., Wang, M.Y., Okuyama, T., 2022. Disrupted social memory ensembles in the ventral hippocampus underlie social amnesia in autism-associated Shank3 mutant mice. Mol. Psychiatry 27, 2095–2105.

Viventi, J., Kim, D.H., Vigeland, L., Frechette, E.S., Blanco, J.A., Kim, Y.S., Avrin, A.E., Tiruvadi, V.R., Hwang, S.W., Vanleer, A.C., Wulsin, D.F., Davis, K., Gelber, C.E., Palmer, L., Van der Spiegel, J., Wu, J., Xiao, J., Huang, Y., Contreras, D., Rogers, J. A., Litt, B., 2011. Flexible, foldable, actively multiplexed, high-density electrode array for mapping brain activity in vivo. Nat. Neurosci. 14, 1599–1605.

Yagi, S., Igata, H., Shikano, Y., Aoki, Y., Sasaki, T., Ikegaya, Y., 2018. Time-varying synchronous cell ensembles during consummatory periods correlate with variable numbers of place cell spikes. Hippocampus 28, 471–483.

Yoshimoto, A., Shibata, Y., Kudara, M., Ikegaya, Y., Matsumoto, N., 2022. Enhancement of motor cortical gamma oscillations and sniffing activity by medial forebrain bundle stimulation precedes locomotion. eNeuro 9.